Impact of heat treatment analysis on the wear behaviour of al-14.2si-0.3mg-tic composite using response surface methodology

Vol. 43, No. 4 (202x) 590-602, DOI: 10.24874/ti.988.10.20.04

Tribology in Industry

www.tribology.rs

RESEARCH

Impact of Heat Treatment Analysis on the Wear Behaviour of Al-14.2Si-0.3Mg-TiC Composite Using Response Surface Methodology

V. Anilkumar[a,b], K.V. Shankar[b,*], M. Balachandran[c,d], J. Joseph[b], S. Nived[b], J. Jayanandan[b], J. Jayagopan[b], U.S. Surya Balaji[b]

[a]*Department of Industrial and Material Science, Chalmers University of Technology, SE-412 96 Göteborg, Sweden,*
[b]*Department of Mechanical Engineering, Amrita Vishwa Vidyapeetham, Amritapuri, India,*
[c]*Department of Chemical Engineering and Materials Science,*
[d] *Centre of Excellence in Advanced Materials and Green Technologies (CoE-AMGT), Amrita School of Engineering, Coimbatore, Amrita Vishwa Vidyapeetham, India.*

Keywords:

Aluminium metal matrix composite
Wear behaviour
T_6 heat treatment
Response surface methodology
Al-Si-Mg-TiC

* Corresponding author:

Karthik V. Shankar
E-mail: karthikvs@am.amrita.edu

Received: 18 October 2020
Revised: 5 December 2020
Accepted: 30 April 2021

A B S T R A C T

Al-14.2Si-0.3Mg Alloy reinforced with hard phased TiC coarse particulates (10 wt-%) was contrived using the liquid metallurgy route. The so fabricated aluminium metal matrix composites was made to undergo solutionising at 525^{0}C for 12 hours in a heat treatment furnace and was subsequently water quenched to room temperature. The developed composite was then kept for age hardening at varying temperatures and time for enhanced tribological properties. A pin on disc Tribometer (ASTM-G99) was utilised to study the wear properties of the fabricated composite. Aging temperature (^{0}C), applied load (N) and Aging time (hours) were chosen as the process parameters for analysing the material's resistance to wear. Using response surface methodology the influence of reinforcement in the wear properties of the composite was studied. The design of the regression equation was prepared and the impact of each experimental parameter was scrutinized. Results depict that with an increase in the aging temperature, aging time and load, there observed a variation in the materials wear properties. The worn-out surface of the metal matrix composite was then investigated with the help of the Scanning Electron Microscope (SEM).

1. INTRODUCTION

Metals that are reinforced with fibres, monofilaments (MF) or particles are called metal-matrix composites (MMCs) [1]. In the manufacturing of pistons and brake drums used in the automotive industry in recent decades, the MMC material promises to provide high performance. Due to its low cost, enhanced stiffness, isotropic properties, high thermal conductivity and great strength, aluminium metal matrix composite (AMMC) is more

commercially applicable among all metal matrix composites. Some MMC's are higher than the base metal in fatigue efficiency and wear resistance [2]. The development of vortex in the metal gives the stircasting method an advantage and thus demonstrates greater wettability between the reinforcement and the molten metal. Agglomeration, improper distribution, and bonding of reinforced matrix elements are issues that can be found during the manufacture of MMCs through liquid metallurgy process [3]. Because of their wide uses in the automotive and aviation industries, the most widely utilised metal matrix is Al, Ti, Mg and their alloys. The composites in which Al is used as the matrix and many reinforced materials like silicon carbide (SiC), titanium carbide (TiC), and graphite are several of the reinforced materials. AMMC is used for characteristics such as low density, great specific strength, strong mechanical properties, low expansion thermal coefficient, improved resistance to corrosion [4], high strength to low weight ratio and extraordinary resistance to temperature [5].

Numerous processing techniques such as stir casting, spray co-deposition, squeeze casting and penetration of liquid metal [6] are used for casting AMMC. The liquid state stir casting method, where reinforcement particles are reinforced into the Al matrix by mechanical stirring, is the easiest manufacturing technique used for AMMC. The advantages of the stir casting method lie in its simplicity, versatility and applicability to large quantities of production [7]. This technique of liquid metallurgy is the most inexpensive of all the routes existing for the fabrication of metal matrix composites. It also lowers the product's final cost [4]. The addition of titanium carbide to (TiC) A356 melt improves the mechanical properties such as hardness and decreases the wear rate of the developed alloys. In Al-Si alloys, TiC is reinforced to enhance the strength at high temperatures, hardness value and to decrease the material expansion coefficient via heat treatment, the surface property of the material is enhanced. In addition, heat treatment tends to improve AMMC's hardness and strength in a better way. The microstructure is gradually influenced by the alleviation of internal stress and AMMC's grain structure is being refined [8].

The study envisaged by various researchers on AMMCs are as follows. An investigation was performed to evaluate the mechanical, sliding wear behaviour and modelling of TiC reinforced LM25 [9]. In this research 10 wt- % of TiC of average size 50 μm was reinforced into the molten metal and the composite was processed through liquid metallurgy route. Response surface methodology was utilised to assess the output of various parameters involved in wear testing. An uniform scattering of the reinforced particle was noted in the Al matrix, resulting in an improvement in the AMMC's hardness and mechanical properties. A research was conducted to analyze the 3-body abrasive wear characteristics of functionally graded Aluminium reinforced with boron carbide (B_4C) [10]. Horizontal centrifugal casting was used to process the alloy. The study showed that the distance from the outer periphery of the cast sample showed minimum wear rate is attributed to presence of higher reinforcement particles. The specimens were subjected to wear tests on various loads and speeds. SEM analysis was used to characterise the worn-out surface of the samples and to analyse the wear mechanism. In an investigation conducted by N Radhika [11], on the heat treatment analysis of LM13/B_4C, it was noted that the ageing cycle shows an important improvement in the wear performance of the composites. The wear testing parameters were aging temperature, load and ageing period. Using a liquid metallurgy route, the cast samples for the study were contrived and the molten composite mixture was poured into a centrifugal casting chamber The mould was revolved for 5 hours at 525° C and aged at various temperatures. A research was conducted to determine the abrasive wear characteristics of In situ TiC reinforced with Al-Cu matrix. Results showed a siginificant improvement in the abrasive wear and mechanical properties of the composite compared to the parent alloy [12]. A research was performed on the hardening and recrystallization of Al-4.5Cu-1.5Mg precipitation. The alloy was strengthened by TiC nanoparticles [13]. It is noted that 0.2 wt-% of TiC / Ti refines the average grain size by reducing the grain size to 76 μm.

A research was conducted to analyse the wear behaviour of LM13 reinforced with 12 wt-% of TiO_2 and 3 wt-% of MoS_2 using response surface

methodology [14]. The hybrid metal matrix composite was contrived via the technique of stir casting. It was noted that a surge in the sliding velocity and load increased the value of wear rate for the base alloy and the composite. A research was carried out to study the tribological behaviour of SiC_p-reinforced Al6061 [15].

From the above discussions, it can be noted that, the effect of heat treatment analysis on TiC reinforced Al alloy has not been investigated. Hence the existing study deals with the manufacturing of Al-14.2Si-0.3Mg-10 wt%/TiC (Hypereutectic composite) by the process of liquid metallurgy and to study the tribological behaviour using response surface methodology because of its vast applications in the manufacturing of pistons and liners in automobile industries.

2. MATERIALS SELECTION

For the present investigation, A356 (Al-7Si-0.3Mg) was selected from among the various grades of aluminium alloy as this alloy is used in the manufacturing of pistons and other structural application in automobile and aerospace industry. To achieve a hypereutectic composition, the wt-% of Si content in the A356 alloy was increased to 14.2 wt-%. This composition was chosen for the preparation of MMC due to the use of hypereutectic aluminium alloy in the automotive industry. In this analysis, TiC with an average micron size of 33-35µm as shown in Fig. 1 was used as a reinforcement. The EDS analysis of the TiC is shown in Fig. 2 and it comfirms the purity of the reinforcement.

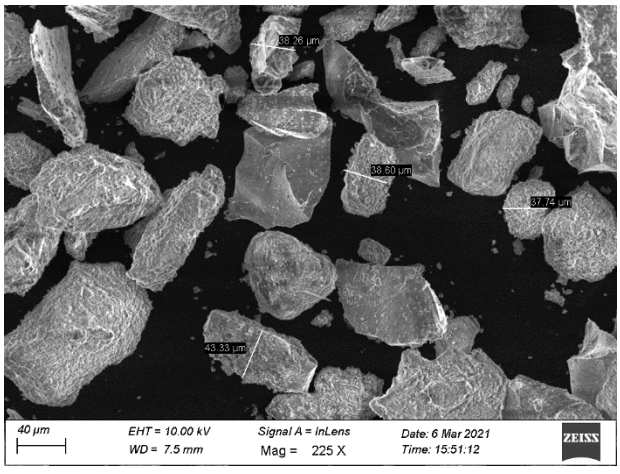

Fig 1. SEM image of TiC.

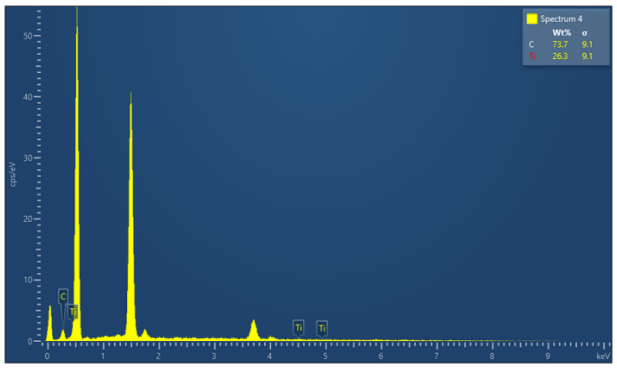

Fig 2. EDS spectrum of TiC powder.

TiC was selected as the reinforcement, among other ceramic reinforcements, owing to its high wear resistance and value of hardness. The density was found to be 2.67 g/cm^3 and 4.93 g/cm^3, respectively, for A356 and TiC. The material for manufacturing the permanent mould was oil-hardened non-shrinkage steel (OHNS), as shown in Fig 3.

Fig 3. OHNS permanent mold.

3. EXPERIMENTAL METHODOLOGY

The A356 was used as an ingot for melting in this current analysis. A required quantity of wt- percent of Si was alloyed into the molten metal to obtain the hypereutectic composition and the melt was poured into a permanent mould to obtain cast rods. To confirm the elemental composition of the hypereutectic Al alloy, optical arc spectroscopy was performed on the cast rods. The wt- % composition of hypereutectic Al alloy is depicted in Table 1.

The cast rods of hypereutectic composition was taken in a clay graphite crucible and was positioned inside an electric arc furnace chamber equipped with a mechanical stirrer as depicted in Fig 4.

Table 1. Wt-% of the composition of hyperutectic Al alloy.

Elements	Wt-% composition
Al	Bal.
Si	14.2
Mg	0.3
Cu	0.1
Fe	0.6
Ni	0.1
Pb	0.1
Sn	0.05
Al	Bal.

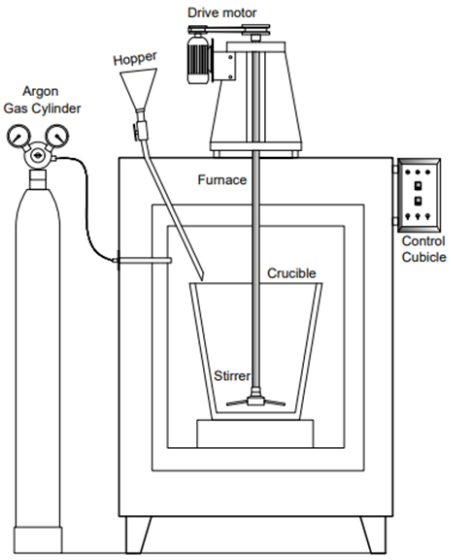

Fig. 4. Stir casting furnace.

The 10wt-% TiC reinforcement was simultaneously preheated in a muffle furnace at a temperature of 300° C to eradicate the moisture content and to improve the wettability of the reinforcement with the matrix. The melting of the composite mixture was carried out in an inert argon atmosphere. In order to minimise oxidation, prevent chemical reaction between the reinforcement and the matrix, and obtain defect-free cast rods, the inert atmosphere was favoured during melting. The required amount of TiC was added into the melt within the crucible and 1 wt-% of Mg was added. By adding Mg, the wettability of the reinforcement ceramic particle with the matrix would enhance by increasing the surface energy of the reinforcement by reducing the surface tension [10]. The added Mg also interacts with the oxygen present in the layer that thins the reinforced particle's gas layer, thus reducing the propensity to agglomerate and increasing the matrix wettability of the particle. To obtain a homogeneous distribution of the particles in the molten metal, the mixture is then stirred for 10 minutes at 250 rpm [10]. At a temperature of 500° C ± 10° C, the die used for the present research was preheated. The molten metal was then poured at a temperature of 760° C ± 10° C into a die coated with Lubrikote 140 preheated die to achieve cast rods of diameter16 mm and length of 150 mm, as shown in Fig 5. As depicted in Fig 6, the cast rods were then machined to a dimension of 15 mm in diameter and 140 mm in length.

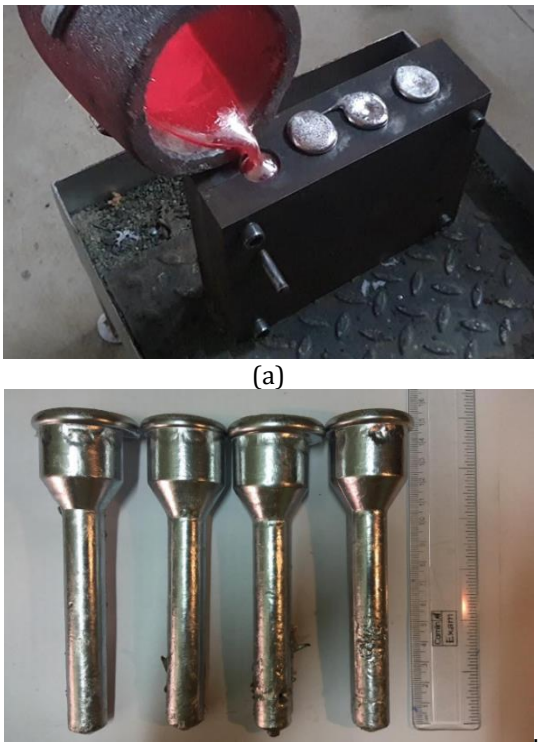

(a)

(b)

Fig. 5. (a) Pouring of molten metal (b) as-cast rods.

Fig. 6. Machined specimen.

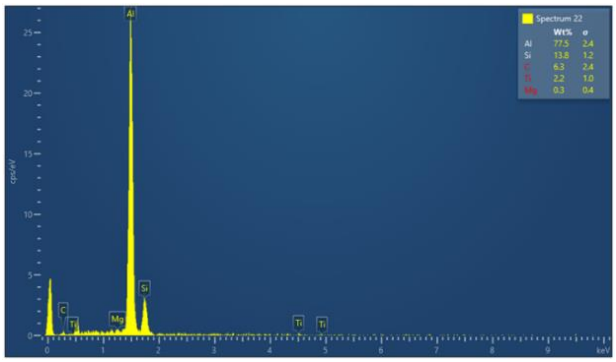

Fig. 7. EDS spectrum showing the presence of TiC.

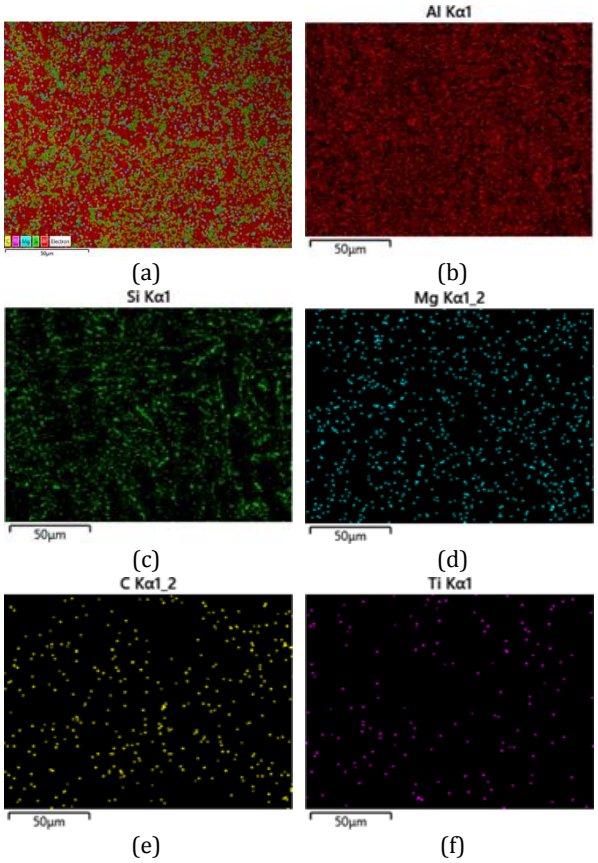

Fig. 8. Elemental mapping of the cast composite.

Samples were machined from the cast rods for metallographic inspection and wear testing. Energy dispersive spectroscopy (EDS) study was performed on the sample to confirm the presence of TiC in the composite. 6 spots on the specimen were taken in various areas and an average value was determined. The EDS spectrum of the cast composite confirms the presence of TiC as shown in Fig. 7. Fig 8 shows the morphological elemental mapping of the cast composite by scanning electron microscopy (SEM) with energy dispersive X-ray spectrometry (EDS). Figure 8 shows that all elements in the matrix are distributed uniformly. Carl Zeiss metallurgical microscope was utilized to study the distribution of the ceramic particles in the Al matrix.

4. HEAT TREATMENT PROCESS

The Heat treatment process was designed to comply to the standards mensioned in the American Society of Materials Handbook. The heat treatment process generally involoves solutionizing, water quenching, and ageing. Solutionisation of the cast composites were carried out in a heat treatment furnace at 525° for 12 hours [16] and the specimens were water quenched at 30° C. The quenched samples were then machined and aged at 151,153 and 155° C for 1, 3, 4, 5 hours [16] and the aged specimens were allowd to cool at room temperature.

5. MICROSTRUCTURAL ANALYSIS

In accordance with the standard metallographic technique to examine the microstructure, the specimens from the heat-treated composite were machined. To achieve a good surface finish, the specimens were polished using a linear polisher followed by a SiC emery sheet of 1/0 and 2/0. Using a double-disc automated polishing unit, the machined specimens were then polished using Al_2O_3 solution to achieve a fine surface finish. For the polished samples, Kellers' reagent was used as an etchant. Furthermore, through a Carl Zeiss metallurgical optical microscope, the microstructure of the etched samples was viewed. The as-cast microstructure of the Hypereutectic Alloy Al-Si-Mg is shown in Figure 8. From the figure, It depicts thecomplete nodular eutectic Si. A vortex flow is produced inside the molten metal at the time of stirring, which absorbs the ceramic particles into the melt rather than allowing them to float on the molten metal's surface. In addition, preheating conducted on the ceramic reinforcement and an addition of 1 wt-% of Mg improved the wettability of the reinforcement with the Al matrix, thereby avoiding the agglomeration factor during casting time.

6. RESPONSE SURFACE METHODOLOGY

For a problem with several explanatory variables, response surface methodology is a tool used to obtain an optimum result. This approach helps to minimise the number of experiments for

parameters such as load, time and temperature using permutation and combination applications. For predicting the answer to a different combination of parameters, fitting experimental data, estimating regression coefficients and testing the adequacy of the fitting model, a series of steps can be used [17-19]. At dry sliding wear conditions the experiment was performed. In response surface analysis, the dependence of the response y on the influencing factors (x_i) can be modelled with a 2nd order polynomial equation of the form

$$y = \beta_0 + \sum \beta_i x_i + \sum \beta_{ii} x_i^{\,2} + \sum \beta_{ij} x_i x_j \quad (1)$$

where y is the response and xi represent the factors or independent variables considered in the experimental design. When normalized centred representations are used to signify the factor levels, β_0, β_i, β_{ii} and β_{ij} are the mean values of responses, linear, quadratic and interaction constant coefficients respectively. In this case, specific wear rate is the response y whereas load, aging temperature and aging time are the independent variables. Each independent variable or factor was varied at 3 levels in the experimental design. With the help of Minitab software, by means of Face Centred Central Composite Design (FCCD), a type of RSM method, 20 experiments were generated for parameter load (10, 20,30N), aging temperature (151,153 and 155° C) and aging time (3,4,5hrs). The sliding distance, sliding velocity and Track diameter were constant at 1000 m, 1m/s and 90mm. The wear testing factors used for the test are tabulated in Table 2.

Table 2. Wear testing parameters

Factors	Level		
Load (N)	10	20	30
Ageing temperature (°C)	151	153	155
Ageing time (hours)	3	4	5

7. DRY SLIDING WEAR TEST

From the cast composite, the specimen size of 10 x 10 x 10 mm was machined and the sliding wear test was conducted as per ASTM G99 was carried out according to the experimental design obtained by adopting face centred composite design (FCCD). The wear testing was carried out in a pin –on –disc tribometer as shown in Fig. 9. The test was conducted in the air in the dry sliding state. During the wear test, the room temperature was noted to be 30° C with a relative humidity of 45 ± 15%. The specimen was kept firmly in contact with the EN 32 counter face disc of hardened steel with a Rockwell hardness of 65HRC in a specimen holder. By applying the applied load through a lever mechanism, the cast specimen was held in direct contact with the counterface disc. Before and after the procedure, the mass of the cast composite specimen was measured using an electronic weighing system with an accuracy of 0.1 mg. The specific wear rate has been evaluated using the equation (2). For each experimental setting, the wear experiments were repeated 5 times, the average value of specific wear rate was calculated and reported

$$W = (M / \rho D) / Load \quad (2)$$

where, W=Specific wear rate in mm^3 / Nm, M=mass loss in g, ρ=density in g / mm^3, D=sliding distance in m and Load in Newton.

As per the Archard's wear adhesion theory [20], it is found that the wear rate is directly proportional to load and sliding distance. The wear coefficient (K) value for all the experiments conducted in this investigation was calculated using the equation (3)

$$W = K \times L \times D \quad (3)$$

where W is the specific wear rate in (mm^3/Nm), K is the wear coefficient, L is the normal load in (N) and D is the sliding distance in (m).

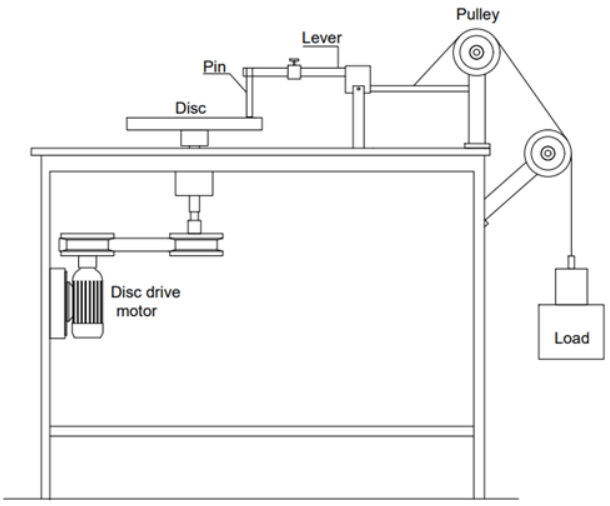

Fig. 9. Pin-on-disc wear testing apparatus.

8. RESULTS AND DISCUSSIONS

8.1 Morhological analysis

The as-cast dendritic structure of Al-Si-Mg hypereutectic aluminium alloy is depicted in Fig 10. It depicts the the complete nodular eutectic Si. Fig 11 (a) depicts the microstructural image of hypereutectic composite in the as-cast condition showing the uniform distribution of 10wt-% of TiC. It can be inferred from Figure 11 (a) that no form of agglomeration of the reinforcement has taken place in the Al matrix. Figure 11 (b) depicts the microstructure of heat-treated hypereutectic composite. It can be noted from the figure that the TiC particles show precipitates enriched in Mg or Si interfaces with the Al matrix. EDS analysis conducted on the heat-treated samples confirms the presence of solute particles like Mg or Si, especially in the Al-TiC interface. Fig 12 shows the EDS pattern of the heat-treated composite.

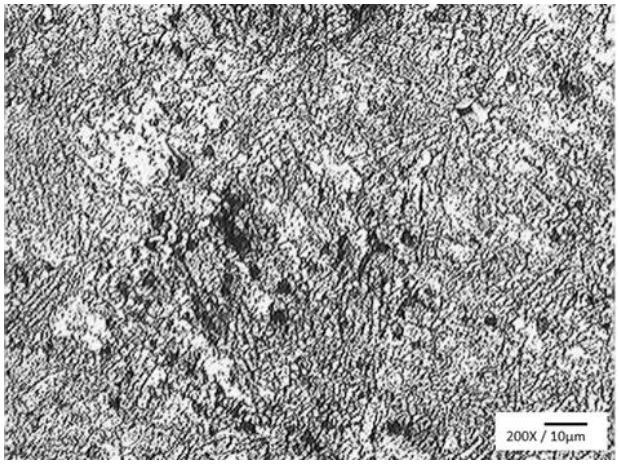

Fig. 10. As-cast structure of Al-Si-Mg hyperutectic alloy.

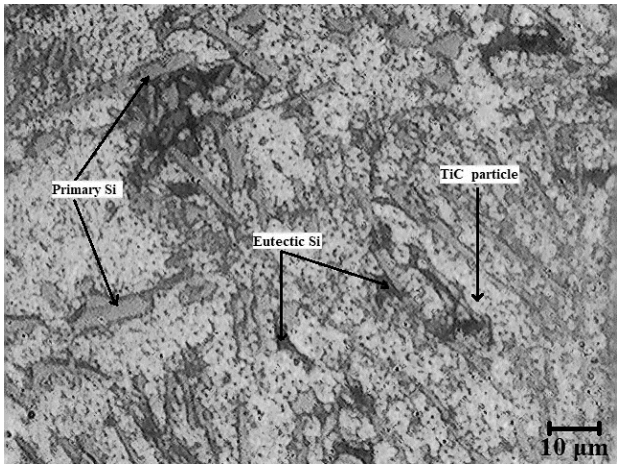

(a)

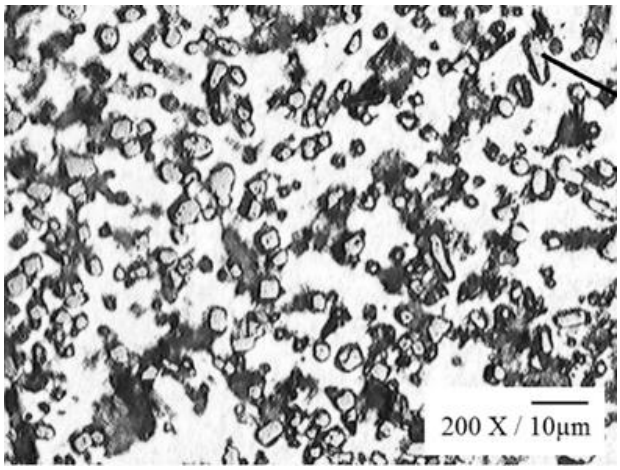

(b)

Fig. 11. Microstructure of hypereutectic composite (a) Non heat-treated (b) Heat Treated.

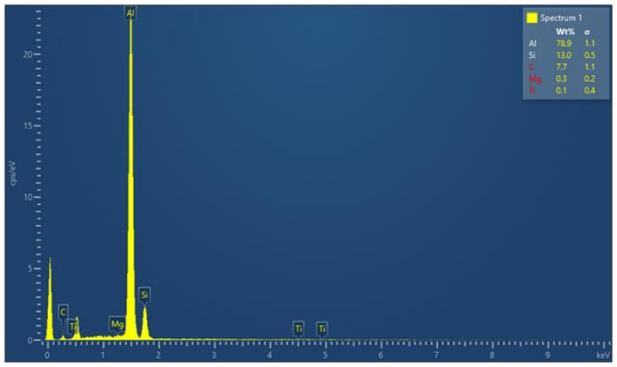

Fig. 12. EDS spectrum of heat treated composite.

8. 2 Analysis of Specific Wear Rate

Table 3 illustrates the wear rate values obtained for various test runs and Table 4 shows the regression coefficient values of the specific wear rate.

For the attained model, the values of R^2 and adj R^2 are 53.71% and 37.18% respectively. This shows that the R^2 value of 53.71% of the difference in the response can be described by the combination of settings of the three parameters. This may be due to the influence of uncontrollable factors such as heat dissiaptation during wear tests. Higher the R^2 values, the better the polynomial is for describing the behavior of the system. The model is valid only within this range of parameters (load, aging temperature, aging time). The regression coefficients are used to construct the model which is displayed in equation (1).

Table 3. Displays the wear rate values.

C1	C2	C3	C4	C5	C6
Sl no	**Applied load (N)**	**Aging temperature (^{0}C)**	**Aging time (hrs)**	**Specific wear rate ($\times10^{-4}$ mm^3/Nm)**	**Hardness Value (Hv)**
1	10	153	4	4.10	151
2	10	155	5	3.69	159
3	20	151	4	2.46	164
4	30	151	3	9.33	145
5	10	151	3	1.12	190
6	20	153	3	2.57	162
7	20	155	4	2.80	161
8	10	155	3	2.24	167
9	20	153	4	1.68	180
10	20	153	4	2.24	167
11	30	155	5	2.11	170
12	20	153	5	1.27	185
13	30	153	4	2.74	161
14	20	153	4	1.87	176
15	30	151	5	1.87	175
16	20	153	4	1.87	176
17	10	151	5	2.99	157
18	20	153	4	2.99	157
19	20	153	4	4.66	151
20	30	155	3	2.49	164

Table 4. Displays the regression coefficients obtained.

Source	DF	Adj SS	Adj MS	F -Value	P -Value
Model	5	0.000000	0.000000	3.25	0.037
Linear	3	0.000000	0.000000	1.24	0.331
Applied load(N)	1	0.000000	0.000000	0.99	0.337
Aging temperature(^{0}C)	1	0.000000	0.000000	1.00	0.333
Aging time(hours)	1	0.000000	0.000000	1.74	0.209
2-Way Interaction	2	0.000000	0.000000	6.26	0.011
Applied load(N)*Aging temp(^{0}C)	1	0.000000	0.000000	4.54	0.051
Applied load(N)*Aging time(hrs)	1	0.000000	0.000000	7.97	0.014
Error	14	0.000000	0.000000		
Lack of fit	9	0.000000	0.000000	1.80	0.269
Pure error	5	0.000000	0.000000		
Total	19	0.000001	0.000000		

$$\text{Specific Wear Rate (mm}^3\text{/Nm)} = -0.01340 + 0.000865L + 0.000083T + 0.000221t - 0.000005L\times T - 0.000014\, L \times t \quad (4)$$

Where, L is Applied load in N, T is Aging temperature in ^{0}C, t is aging time in hours.

The linear and 2-way interactions affect the wear behaviour of the composite. Equation (4) indicates that positive sign parameters affect increasing the wear rate and negative sign parameters affect decreasing the wear rate of the composite.

8.3 Study of variance of specific wear rate

Table 5 displays the importance of terms involved in the contribution of the model and it was found out by using the analysis carried out for a 90% confidence level and a 10% significance level. The analysis can be used to find the

significance of various factors like regression model, linear terms, 2-way interaction terms and lack of fit. P-value is used to find whether the results are statistically significant or not. The hypothesis test is statistically significant if P-value is less than the importance level (α<0.1). For further analysis, the terms with P values higher than α is removed from the model.

Table 5. Regression analysis for wear.

Term	Effect	Coef	SE-coef	T-value	P-value	VIF
Constant		0.000285	0.000031	9.14	0	1
Applied load(N)	0.000088	0.000044	0.000044	0.99	0.337	1
Aging temperature(^{0}C)	-0.000089	-0.000044	0.000044	-1.00	0.333	1
Aging time(hrs)	-0.000116	-0.000058	0.000044	-1.32	0.209	1
Applied load(N)*aging temperature(^{0}C)	-0.000211	-0.000105	0.000049	-2.13	0.051	1
Applied load(N)*aging time(hrs)	-0.000279	-0.000139	0.000049	-2.82	0.014	1

8.4 Influence of interaction parameters on the responses

The interaction plot for the specific wear rate is depicted in Fig.13

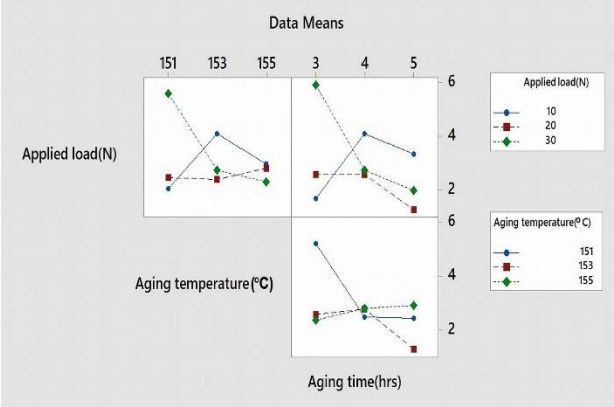

Fig. 13. Interaction Plot for specific wear rate ($\times10^{-4}$ mm^3/Nm).

At 10 N with the gradual surge in ageing temperature, specific wear rate is found to be increasing and then is observed to take a downswing. On the application of 20 N load there is a miniscule decline in wear rate and then a steady increase is observed with increasing ageing temperature. Whilst with 30 N load as ageing temperature climbs up a steep decline in wear rate can be seen. The third factor (ageing time) is maintained at a mid-value with the variation of applied load and ageing temperature. To factor combinations to obtain low specific wear rate as interpreted from Fig. 13 is summarized in Table 6.

For plot [b] X axis is ageing time (hours) and the secondary factor is applied load in N. between 3 hours and 5 hours' time, the ageing time parameter is varied in steps of 1 hour. At an applied load of 10N there is a steady surge in specific wear rate and then a downward trend can be visualized with the growth of ageing time in hours. A sizeable variation in specific wear rate can be seen with an increase in applied load. When the load is increased to 20 N there isn't much fluctuation in specific wear rate with respect to increase ageing time between 3 hours to 4 hours, but a downswing in specific wear rate is observed when ageing goes beyond 4 hours. The scenario with 30N is a stark contrast to what is observed with other loads, a steep decline in wear rate when ageing temperature is varied between 3 hours to 4 hours, and then there is a slowdown in reduction of specific wear rate from 4 hours to 5 hours.

Table 6. Factors ranges for responses of Al-14.2Si-0.3Mg-TiC metal matrix composite.

Response	Objective	Factor ranges			Ref
		Load (N)	Ageing Temperature (°C)	Ageing time (hrs.)	
Specific wear rate	Minimize	10N	151	3	13(a)
		30N	155	5	13(b)
		20N	153	5	13(c)

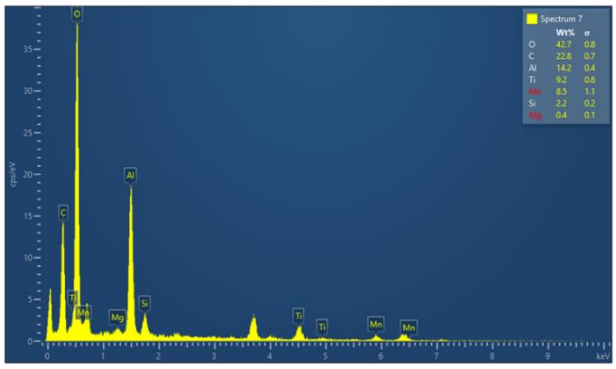

Fig. 14. Mechanically mixed layer.

It can be understood that the resistance to wear of the AMMC increases with increase in load and increase in aging time, which can be attributed to the presence of TiC particles which are hard phased increases the overall strength of the material by exposing more TiC particles when load is increased, and the creation of a layer as shown in Fig. 14, the Mechanical Mixed Layer (MML) and thereby shoots up the resistance to wear [21,22]. The optimum aging time was found to be between 4 hours to 5 hours where it can be noted that the value specific wear rate decreases. To investigate the effect of ageing temperature at first the low-level load of 10 N is applied and the ageing temperature is varied from 151° C to 155° C and a rapid decline in the specific wear rate is observed as the temperature is increased from 151-153° C and then it stabilizes. On a stark contrast to what is observed with 10N load, under the application of 20 N load between 151-153 the wear rate doesn't seem to fluctuate a lot, but after 153 it drops down in a steady fashion. Whilst for 30 N load the specific wear rate is noted to be increasing in a small but steady way. At lower aging temperatures mainly 151° C the TiC reinforced in the Aluminium metal matrix composite (AMMC) exist in granular and forms clusters [11] which signifies the lower wear resistance but as the aging temperature is increased to 153° C due to thermal diffusion at phase interface, it is found to have a refined size and morphology of the coarse grain TiC particles, also it forms a uniformly distributed phase within the matrix this uniformity within the matrix will improve the strength and thereby wear resistance. It can be inferred from the analysis that a small change in ageing temperature can create a dramatic change in the way the material reacts to wear [23,24].

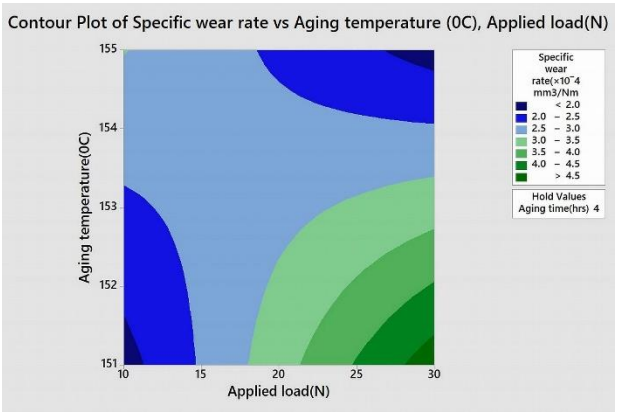

(a)

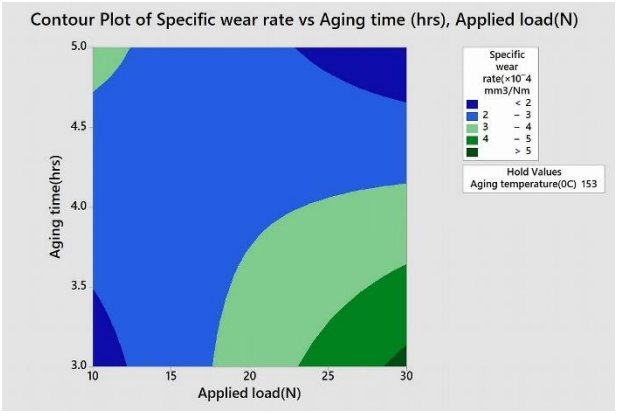

(b)

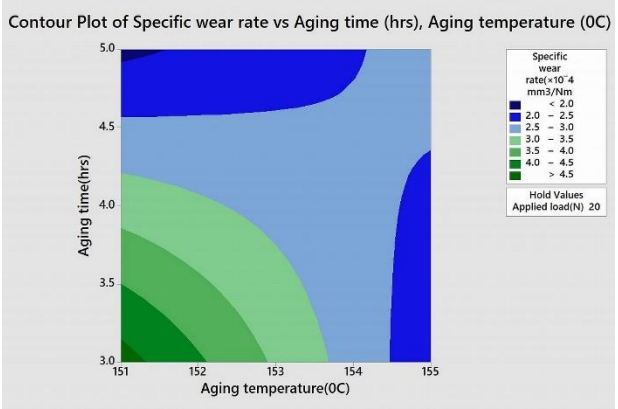

(c)

Fig. 15. Contour Plots of Specific Wear rate(mm^3/Nm).

Fig 15 (a), (b), (c) depicts the contour plot which helps us conceive how the specific wear rate varies with applied load, ageing time and ageing temperature. In a contour plot the third factor is held constant while the other two are varied at once and the corresponding change in response of the system is delineated. On further scrutiny on contour plots it can be inferred that for both 10 N load for 3 hours at 151 and 30 N at 155 for 5 hours yields the lowest specific wear rate values for the latter case where load is increased along with ageing temperature and

aging time the specific wear rate is found to be on a downswing. This can be due to the fact that as aging time is augmented, the age hardening happens which reaches a peak level and fine coherent precipitates of Mg_2Si are formed which helps in increasing the strength of the Aluminium Metal Matrix Composite thereby reducing specific wear rate [11]. The legend given on right hand side of the figure, representing contour plot delineates different colour tone for representing the specific wear rate with the darker variation of blue pointing towards the lowest specific wear rate region and darkest green representing regions with highest specific wear rate. With the lighter variants of blue and green illustrating the mid-level regions. Section (a) of the contour plot maps aging temperature (hours) vs applied load (N) the colossal region represented by a lighter shade of blue is where specific wear rate is 2- 3 x 10^{-4} (mm^3/Nm) whereas section (b) illustrates aging time (hours) vs applied load (N) and (c) depicts aging temperature and aging time (hours), it can be inferred that highest wear rate is observed when aging time is 3 hours and applied load is 30N. Lowest wear rate is when aging time is 5 hours and applied load is 30 N. This is because of particle hardening that strengthens the material by forming precipitates. Towards the upper half of the map and lower left portion of the map corresponds to the low specific wear rate.

9. ANALYSING OF WORN OUT SURFACE USING SEM

Using SEM, the worn out surface of the composite specimen was analyzed and the results inferred are given below. The SEM images were taken at 100X magnification, Fig 16 (a-c) shows SEM images of specimens under different load (10N,20N,30N) with constant ageing temperature (155^0C) and ageing time (5 hours). in Fig 16 (a) A_1 represents the wear track, B_1 represents the debris, C_1 represents shallow grooves, severe delamination is observed in this specimen when 10 N load is applied with 5 hrs ageing time, the depth of shallow grooves can also be observed to be higher that both (b) and (c). with increase in load, the material removal due to rate of wear is found to be decreasing this is owed to the development of Mechanical Mixed Layer (MML), A_2,B_2,C_2 on figure (b) and A_3,B_3,C_3 on figure (c) represents wear track, debris, and shallow grooves in order, it is visible that the depth of shallow grooves is decreasing as the load is increasing, and fewer number of debris can be found this is due to MML formation and partly due to T6 heat treatment that was done on the specimen.

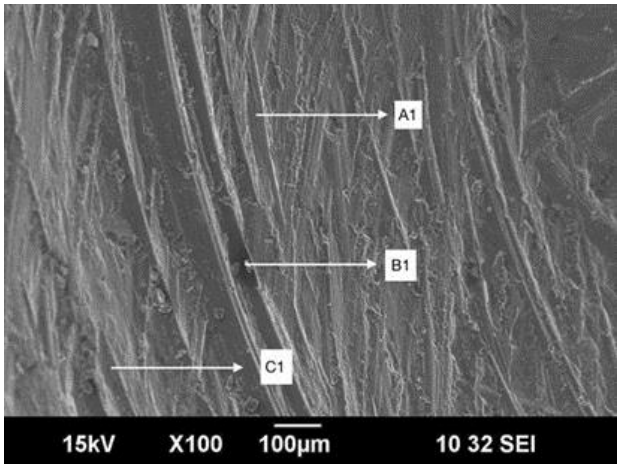

(a)

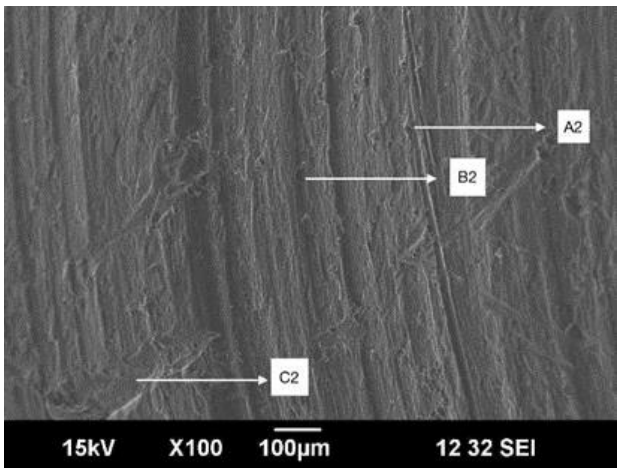

(b)

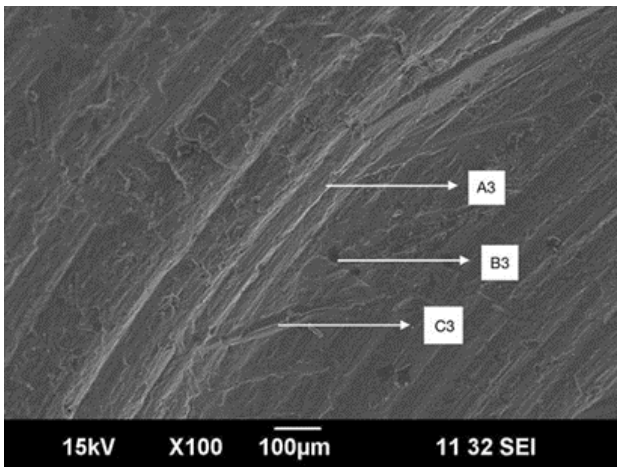

(c)

Fig. 16. (a-c): SEM images of the worn out composite specimen.

10. CONCLUSION

A356 Al alloy with added Silicon content to take it to hypereutectic composition along with 10 wt% of TiC was contrived using Stir-casting technique. The so obtained AMMC was subjected to T6 heat treatment for enhanced wear properties. RSM (Response surface methodology) was employed in studying the wear properties of the specimen, a RSM model was developed for conducting the study and following conclusion were noted.

- Materials Optimum resistance to wear was observed to be when the AMMC was subjected to a load of 30N, a higher aging temperature of 155^0C and an aging time of 5 hours.
- The optimum values of wear factors necessary to obtain minimum wear rate was calculated using RSM model.
- The SEM images revealed that the formation of shallow groves and debris reduced as the load increases.

REFERENCES

[1] G.W. Walkiden, *The Noble Metals, Corrosion–Metal/Environment Reactions*, Elsevier, 1979

[2] M.K. Surappa, *Aluminium matrix composites: Challenges and opportunities,* Sadhana, vol. 28, iss. 1-2, pp. 319-334, 2003, doi: 10.1007/BF02717141

[3] P.V. Reddy, G.S. Kumar, D.M. Krishnudu, H.R. Rao, *Mechanical and wear performances of aluminium-based metal matrix composites: A review*, Journal of Bio- and Tribo-Corrosion, vol. 6, iss. 3, 2020, doi: 10.1007/s40735-020-00379-2

[4] D.S. Prasad, A.R. Krishna, *Tribological properties of A356.2/RHA composites*, Journal of Materials Science and Technology, vol. 28, iss. 4, pp. 367-372, 2012, doi: 10.1016/S1005-0302(12)60069-3

[5] A.C. Petare, N.K. Jain, *A critical review of past research and advances in abrasive flow finishing process*, International Journal of Advanced Manufacturing Technology, vol. 97, iss. 1-4, pp. 741-782, 2018, doi: 10.1007/s00170-018-1928-7

[6] S. Subramanian, B. Arunachalam, K. Nallasivam, A. Pramanik, *Investigations on tribo-mechanical behaviour of al-Si10-Mg/sugarcane bagasse ash/SiC hybrid composites*, China Foundry, vol. 16, iss. 4, pp. 277-284, 2019, doi: 10.1007/s41230-019-8176-9

[7] J. Singh, C.S. Jawalkar, R.M. Belokar, *Analysis of mechanical properties of AMC fabricated by vacuum stir casting process,* Silicon, vol. 12, iss. 10, 2020, doi: 10.1007/s12633-019-00338-8

[8] S. Nanjan, J.G. Muralia, *Analysing the mechanical properties and corrosion phenomenon of reinforced metal matrix composite*, Materials Research, vol. 23, no. 2, 2020, doi: 10.1590/1980-5373-MR-2019-0681

[9] N. Radhika, R. Raghu, *Prediction of mechanical properties and modeling on sliding wear behavior of LM25/TiC composite using response surface methodology*, Particulate Science and Technology, vol. 36, iss. 1, pp. 104-111, 2018, doi: 10.1080/02726351.2016.1223773

[10] N. Radhika, R. Raghu, *Three body abrasion wear behaviour of functionally graded aluminium/B4C metal matrix composite using design of experiments*, Procedia Engineering, vol. 97, pp. 713-722, 2014, doi: 10.1016/j.proeng.2014.12.301

[11] L.V. Priyanka Muddamsetty, N. Radhika, *Effect of heat treatment on the wear behaviour of functionally graded LM13/B4C composite,* Tribology in Industry, vol. 38, no. 1, pp. 108-114, 2016.

[12] A. Kumar, P.K. Jha, M.M. Mahapatra, *Abrasive wear behavior of in situ tic reinforced with al-4.5%Cu matrix*, Journal of Materials Engineering and Performance, vol. 23, iss. 3, pp. 743-752, 2014, doi: 10.1007/s11665-013-0836-0

[13] B. Zhao., Q. Cai, J. Cheng, S. Yang, F. Chen, Investigation on recrystallization and precipitation behaviors of Al-4.5Cu-1.5 Mg alloy refined by ti-supported TiC nanoparticles, Journal of Alloys and Compounds, vol. 800, pp. 392-402, 2019, doi: 10.1016/j.jallcom.2019.05.323

[14] R. Jojith, N. Radhika, *Mechanical and tribological properties of LM13/TiO2/MoS2 hybrid metal matrix composite synthesized by stir casting,* Particulate Science and Technology, vol. 37, iss. 5, pp. 566-578, 2019, doi: 10.1080/02726351.2017.1407381

[15] V.C. Uvaraja, N. Natarajan, I.S. Rajendran, K. Sivakumar, *Tribological behavior of novel hybrid composite materials using taguchi technique,* Journal of Tribology, vol. 135, iss. 2, 2013, doi: 10.1115/1.4023147

[16] E.L. Rooy, *Introduction to Aluminum and Aluminum Alloys,* in Properties and Selection: Nonferrous Alloys and Special-Purpose Materials, ASM Handbook, pp. 618-626, 1990, doi: 10.31399/asm.hb.v02.a0001057

[17] M.K. Pitchan, S. Bhowmik, M. Balachandran, M. Abraham, *Process optimization of functionalized MWCNT/polyetherimide nanocomposites for aerospace application,* Materials and Design, vol.

127, pp. 193-203, 2017, doi: 10.1016/j.matdes.2017.04.081

[18] M. Balachandran, S. Devanathan, R. Muraleekrishnan, S.S. Bhagawan, *Optimizing properties of nanoclay-nitrile rubber (NBR) composites using face centred central composite design*, Materials and Design, vol. 35, pp. 854-862, 2012, doi: 10.1016/j.matdes.2011.03.077

[19] P. Chinnaiyan, S.G. Thampi, M. Kumar, M. Balachandran, *Photocatalytic degradation of metformin and amoxicillin in synthetic hospital wastewater: Effect of classical parameters,* International Journal of Environmental Science and Technology, vol. 16, iss. 10, pp. 5463-5474, 2019, doi: 10.1007/s13762-018-1935-0

[20] R. Duraisamy, S.M. Kumar, A.R Kannan, N.S. Shanmugam, K. Sankaranarayanasamy, M.R. Ramesh, *Tribological performance of wire arc additive manufactured 347 austenitic stainless steel under unlubricated conditions at elevated temperatures,* Journal of Manufacturing Processes, vol. 56, pp. 306-321, 2020, doi: 10.1016/j.jmapro.2020.04.073

[21] V.A. Kumar, V.V.V. Kumar, G.S. Menon, S. Bimaldev, M. Sankar, K.V. Shankar, M. Balachandran, *Analyzing the Effect of B4C/Al2O3 on the Wear Behavior of Al-6.6Si-0.4Mg Alloy Using Response Surface Methodology*, International Journal of Surface Engineering and Interdisciplinary Materials Science, vol. 8, iss. 2, pp. 66–79, 2020, doi: 10.4018/ijseims.2020070105

[22] E.P. Sreedev, H.K. Govind, A. Raj P, S. Adithyan, H.A. Narayan, K.V. Shankar, M. Balachandran, *Determining the significance of cobalt addition on the wear characteristics of Al-6.6Si-0.4Mg hypoeutectic alloy using design of experiment,* Tribology in Industry, vol. 42, no. 2 ,pp. 299–309, 2020, doi: 10.24874/ti.777.10.19.04

[23] P.D. Srivyas, M.S. Charoo, *Effect of sintering temperature and reinforcement concentration on the tribological behaviors of hybrid aluminum matrix nano composite*, Tribology in Industry, vol. 4, no. 4, pp. 573–591, 2019. doi: 10.24874/ti.2019.41.04.10

[24] M.A. Chowdhury, D.M. Nuruzzaman, B. Roy, K.S. Samad, R. Sarker, A.H.M. Rezwan, *Experimental investigation of friction coefficient and wear rate of composite materials sliding against smooth and rough mild steel counterfaces*, Tribology in Industry, vol. 35, no. 4, pp. 286–296, 2013.